Global Journal of Engineering and Technology Advances
eISSN: 2582-5003
Cross Ref DOI: 10.30574/gjeta
Journal homepage: https://gjeta.com/

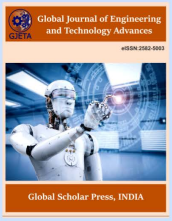

(RESEARCH ARTICLE)

Check for updates

A study of the dependence of the 3-phase cage motor maximum torque on the centroid of the rotor bar section

Nelson Oyakhilomen Omogbai *

Department of Electrical Engineering, Nnamdi Azikiwe University, Awka, Anambra State, Nigeria.

Global Journal of Engineering and Technology Advances, 2023, 14(01), 097–106

Publication history: Received on 13 December 2022; revised on 26 January 2023; accepted on 28 January 2023

Article DOI: https://doi.org/10.30574/gjeta.2023.14.1.0019

Abstract

The paper investigates the relative influence of the centroid of the three-phase squirrel cage induction motor rotor bar cross section, on the breakdown (maximum) torque of the machine. The influence of the angle of taper, the top width and the radial depth of the bar section, as established design variables, were also investigated so as to properly situate the degree of influence of the centroid, in comparison; as far as the maximum torque is concerned. The machines were investigated in their steady state operating mode using the equivalent circuit method. The machine learning capabilities of the Least Square Support Vector Machine (LSSVM) was deployed to extract by prediction, information about the likely dependencies between the randomized block of the geometric variables and the maximum torque, and the captured information was stored using the Root Mean Square Error (RMSE) of predictions. The validated results show that the rotor leakage reactance – a part determinant of the maximum torque; tends to show some significant sensitivity to a design change in the centroid of the transverse section of the rotor bar.

Keywords: Centroid; Maximum torque; LSSVM; RMSE; Rotor leakage reactance; Machine learning

1 Introduction

The squirrel-cage induction motor (SCIM) happens to be the most adopted electrical machine for electrical drives [1]. Studies have shown that to improve the performance of a SCIM, several design variables may have to be modified; one of such adjustments being the optimization of the stator and rotor geometries [2]. The rotor slot geometry which can be considered as an independent design parameter, is the most influential factor in defining the torque-speed characteristic of the SCIM, especially when mains fed [2, 3].

It was pointed out in [4] that between the small and large slip zones, mechanical characteristic exhibits a maximum, which corresponds to the highest torque obtained with given stator supply. A large breakdown torque is usually desirable either for high transient torque reserve or for widening the constant power speed range in variable frequency driven SCIMs [5]. A rotor slot shape that is deep and narrow, allows considerable magnetic flux to cross the slot. Large slot depth leads to a rather high rotor leakage inductance and thus a smaller breakdown torque. In [6], it was demonstrated that rectangular bar rotors produced more breakdown torque but less starting torque compared to the machine with stepped shape rotor. Also, in [2], the authors showed that a decrease of the bar reactance by implementing some design modifications like stepping of a portion of the transverse section, corresponds to the enhancement of the breakdown torque while the resistance played a minor role. The work of [7] in part, investigated the relative values of rotor leakage reactance for SCIM's with circular, oval, and rounded trapezoid rotor bar shapes. They discovered that the circular rotor bar has the least value of rotor leakage reactance and the largest flux linkage. Also, in [15] it was established that the rotor leakage reactance X_2 or the maximum torque T_{max} shows significant sensitivity to the design changes made to the taper angle of the transverse section of the rotor bar.

* Corresponding author: Nelson Oyakhilomen Omogbai

In [8], it was highlighted that when the slot width increases, the overall slot permeance decreases as a result. This decreases the slot leakage flux and thus the leakage reactance of the stator or rotor. The farther away from the stator, a rotor bar or part of a bar is located, the greater is its leakage reactance; since a smaller percentage of the bar's flux will reach the stator [16]. In [9], the authors emphasized that as the height of the rotor slot increases, permeance factor and slot inductance increases. Rotor leakage reactance is proportional to the leakage permeance and the torque developed is inversely proportional to rotor inductance [13]. By varying the slot width and height, the slot factor changes [9]. The study in [10] made the observation that the average torque value decreased with increasing slot height value. Leakage flux is increased in narrow teeth because some of the flux is forced to seek alternate paths other than down the lengths of the teeth. Teeth that are too fat necessitate slots that are too narrow and result in slot leakage flux that is too high [11].

The researcher or designer in practice shall by the outcome of this study be able to ascertain one more critical variable of the bar section to focus on for the finetuning of the maximum torque (T_{max}), and together with other essential stator and rotor variables, may become more guided towards the optimal infeed to the computer algorithms/programs; for easier, more efficient and precise realization of distinct machine designs of target performance.

2 Material and methods

The concept of the centroid or geometric center of the rotor bar section isn't a new one in fields like mechanics and mathematics. Assuming a rotor bar cross section symmetrical about the radial axis through *e*, and approximating the bar cross section as a composite shape comprising two semicircles (top and bottom) and a trapezium (in between) as seen in fig 1, the centroid of the bar cross section may be calculated by the method of geometric decomposition thus:

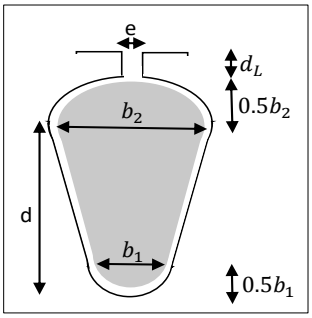

Figure 1 Rotor slot for centroid computation

Let: d_{bar} be the bar radial depth.

The area and centroid of the top semicircle be denoted as A_A and C_A respectively.

The area and centroid of the bottom semicircle be denoted as A_B and C_B respectively, and

The area and centroid of the trapezoidal section be denoted as A_C and C_C respectively.

All centroid depths are calculated relative to the rotor surface, neglecting the lip depth.

From the knowledge of geometry, the centroid of a semicircle of radius r is given as:

$$\frac{4r}{3\pi}, \qquad \text{..... (1.1)}$$

While that for a trapezium of sides a and b and height h is given as:

$$\frac{h}{3}\frac{(b+2a)}{(a+b)}, \text{ (b>a).} \qquad \text{..... (1.2)}$$

Therefore, making use of fig 1;

$$C_A \approx 0.5b_2 - \frac{2b_2}{3\pi} \qquad \text{..... (1.3)}$$

$$C_B \approx d_{bar} + \frac{2b_1}{3\pi} - 0.5b_1 \qquad \text{..... (1.4)}$$

$$C_C \approx 0.5b_2 + \frac{(d-0.5b_1)}{3}\left(\frac{b_2+2b_1}{b_2+b_1}\right) \qquad \text{..... (1.5)}$$

The centroid of the rotor bar cross section relative to the rotor bar surface would then be:

$$C = \frac{C_A A_A + C_B A_B + C_C A_C}{A_A + A_B + A_C} \qquad \text{..... (1.6)}$$

First, two 3ph SCIMs of ratings 100 HP (M1) and 75HP (M2) were run in MATLAB for the purpose of conducting this study and their specifications are given in Table 1.

Second, all variables of machine M1 were kept constant while altering only the geometric parameters of the rotor bar cross section such as the top width (W), the radial depth (D), the angle of taper (T) and of course the centroid; all varied at the same time. The maximum torque responses were recorded against the corresponding varied geometric parameters at each instance of variation, as far as the constraints were not violated and as far as the machine performance indices remain within acceptable limits.

Third, using the tunelssvm, trainlssvm and simlssvm commands from [14], the Least Square Support Vector Machine (LSSVM) was tuned and trained on one part of the collated data (namely, the training dataset) and deployed on the second part (namely, the various blocks of test dataset); to unravel by predicting with the randomized trial procedure, the levels of the underlying dependence that the breakdown torque may likely have on the various randomized blocks of the bar geometric parameters. The randomized blocks were investigated this way using the RMSE of the separate predictions as the metric of comparing the results. The following randomization was applied to the geometric parameter blocks of the rotor bar section:

Lone blocks – W (rotor bar top width), D (bar radial depth), T (angle of taper), and C (radial depth of the centroid of the bar). The centroid is located at point c1 (See fig 2).

Duo blocks – WT, DW. WC, DT, DC, TC.

Triad blocks – WDT, WTC, WDC, and DTC.

Quad block – WDTC.

The most accurate results were then ranked in table 2.

All of the foregoing procedure were repeated with machine M2 which houses rotor bars of completely different design, so as to verify if the observed results are specific to a given machine design or generic within the family of the three-phase SCIMs. The block with the most accurate prediction (least RMSE) for each machine was noted and thoroughly analyzed with the relevant portions of literature, so as to properly situate, prune and finetune the Machine Learning (ML) result.

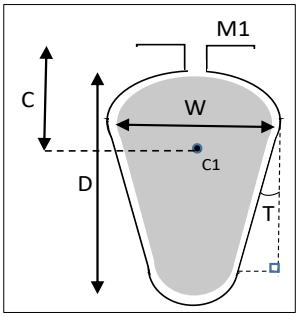

Figure 2 Rotor bar configurations (M1)

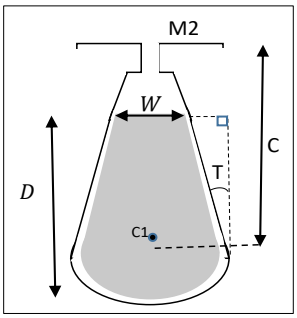

. **Figure 3** Rotor bar configurations (M2)

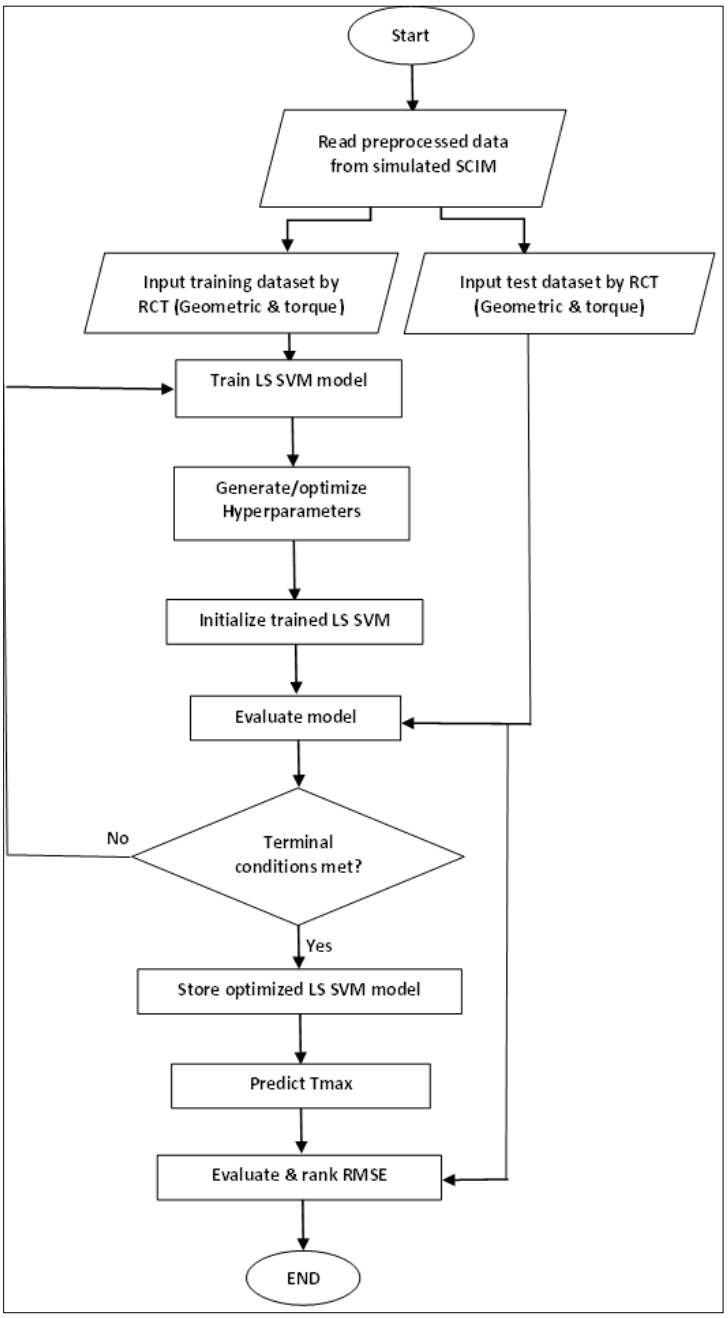

Figure 4 Machine learning flowchart

Table 1 Machine specification

Paramaters	M1	M2
Number of poles (p)	8	6
Number of rotor slots (Sr)	55	55
Number of stator slots (Ss)	72	72
Full load efficiency (EffR) %	91.12268	91.01281
Full load current (I1R) Amps	137.6654	104.0402
Full load power factor (PFR)	0.858292	0.851315
Full load speed (nmR) rpm	738.5339	988.1062
Full load torque (TTdR) N.m	972.3505	545.2107
Starting Torque (Tst) N.m	1211.621	1033.852
Maximum Torque (Tmax) N.m	3368.963	2406.64
X1 (ohms)	0.119191	0.109422
X2pr (ohms)	0.132793	0.136917
Xm (ohms)	3.939174	4.741772
R1 (ohms)	0.035604	0.055372
R2pr (ohms)	0.042764	0.049827
Rc (ohms)	110.508	157.5086

3 Results and discussion

Table 2 Results from machine learning

(M1) Geometric Blocks	(Tmax) RMSE	(M2) Geometric Blocks	(Tmax) RMSE
TC	4.71618E-10	TC	6.2956E-10
WT	5.11776E-10	WT	8.6871E-10
DT	5.25731E-10	DT	1.2359E-09

Table 2 shows that for both machines M1 and M2, the ML tends to put forward the geometric block TC as priority, as far as the influence of bar geometry on the maximum torque is concerned. The introductory section shows that the top width W and depth D of the rotor bar are long established geometric parameters as far as influence on maximum torque is concerned. Also, the significance of the angle of taper T has already been fully discussed in [15], therefore the spot light here shall be on the other half of the TC duo block – C. According to [4];

$$T_{max} = \frac{3pU_{Srms}^2}{2L_{Ye}w_e^2} \qquad \text{…….. (2)}$$

In equation 2, U_S is the peak value of the phase voltages, p is the number of pole pairs, ω_e is the frequency of stator voltages, and currents, and inductance L_{Ye} represent the equivalent leakage inductance of the rotor and stator windings; the rotor being the equivalent two-phase rotor winding that represent the rotor cage and referred to the stator side.

It is noteworthy to observe from Fig 5 that the relationship between the rotor leakage reactance and the maximum torque, for both of the investigated rotors; agrees with equation 2.

$$T_{em} \alpha \phi . I_2 . (rotor\ power\ factor) \ldots\ldots\ldots\ldots\ldots\ldots (3)$$

The account in [12] gives support to the X_2/Torque relation of Fig 5 when he pointed out that a rise in X_2 connotes a drop in the rotor circuit power factor which means a decrease in torque production (T_{em}) according to expression 3, where ϕ *and* I_2 are respectively the airgap flux and rotor current.

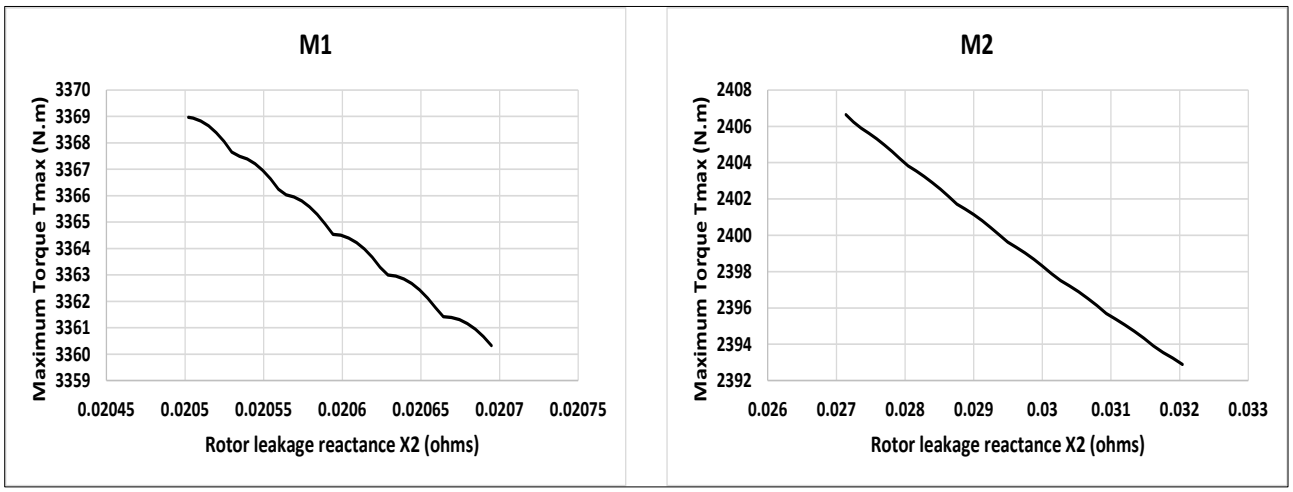

Figure 5 Influence of the rotor leakage reactance on the maximum torque (Rotor bar of M1 & M2)

Further, [16] revealed that the farther away the rotor is located from the airgap, the less its field is magnetically coupled to the stator field and thus the more the magnitude of the leakage flux and thus the greater the value of X_2. The strength of magnetic coupling between the stator and rotor windings is described by the coefficient of inductive coupling k, which varies inversely with the distance between both windings and consequently with the level of the leakage flux too [4]. The distance of an object from a reference could be taken as the distance of its centroid from that reference because the centroid is commonly accepted as the center of mass of an object of homogenous mass and a very good measure of the spatial coordinates of that object [17]. Therefore, we may compare the distance of different rotor bars from their respective airgaps by comparing the radial depths of their centroids from their respective airgaps. From the simulation of machines M1 and M2, the relation in fig 6 obtains.

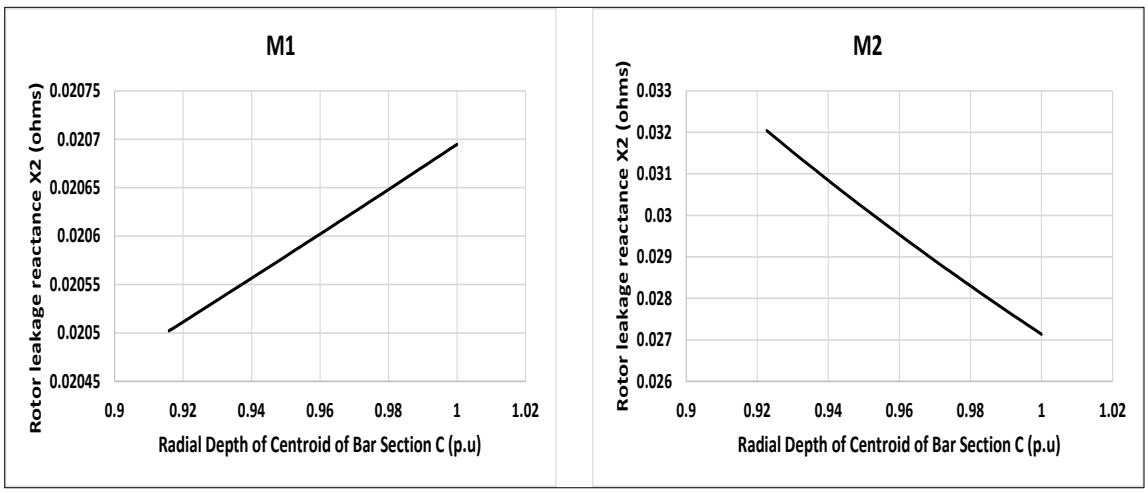

Figure 6 Influence of the radial depth of centroid on the rotor leakage reactance (M1 & M2)

Fig 6 suggests that M1 agrees with the argument in [16] i.e., rotor, X_2 increases with the radial depth of the centroid (C) of the rotor section; but for M2 rotor, it shows an inverse relation. This latter inverse relation between C and X_2 for M2 rotor is inconsistent with literature from the standpoint of the strength of magnetic coupling between the stator and

rotor fields. This observation could be explained from the viewpoint that during the simulation, as T drops, C increases and X_2 tends to decrease for reasons most likely pertaining to the reluctance of the cross-slot path; a trend that is largely influenced by the narrowness (more or less the angle of taper) of the rotor slot or bar [15]. This perhaps suggests that the changes being observed in X_2 and hence T_{max} for M2, are most likely not a function of the design changes made to C.

To highlight the influence of parameter C, the work done in [1] is a case in view. They advanced their earlier study on the stepped bar and went further to make a uniform bore through the narrow section of the stepped bar in such a way as to increase the thickness of this section of the rotor bar in comparison with same section in the case without the bore (implying a decrease in the distance of the centroid from the airgap); and observed that the leakage reactance of the rotor decreased and consequently, the T_{max} increased. They also observed that just decreasing the area of the same section by increasing only the size of the bore (implying an increase in the distance of the centroid from the airgap); led to a decrease of the T_{max}. Note that this bore made through the bar section seems to be an inadvertent move by the authors at shifting the position of the centroid of the bar. These sorts of geometric modification do alter the coupling coefficient between the stator and rotor windings [4], which goes on to alter the leakage flux level and ultimately affecting the T_{max}.

The relation observed in fig 6 is further buttressed in fig 7, as the C/T_{max}.relation depicts.

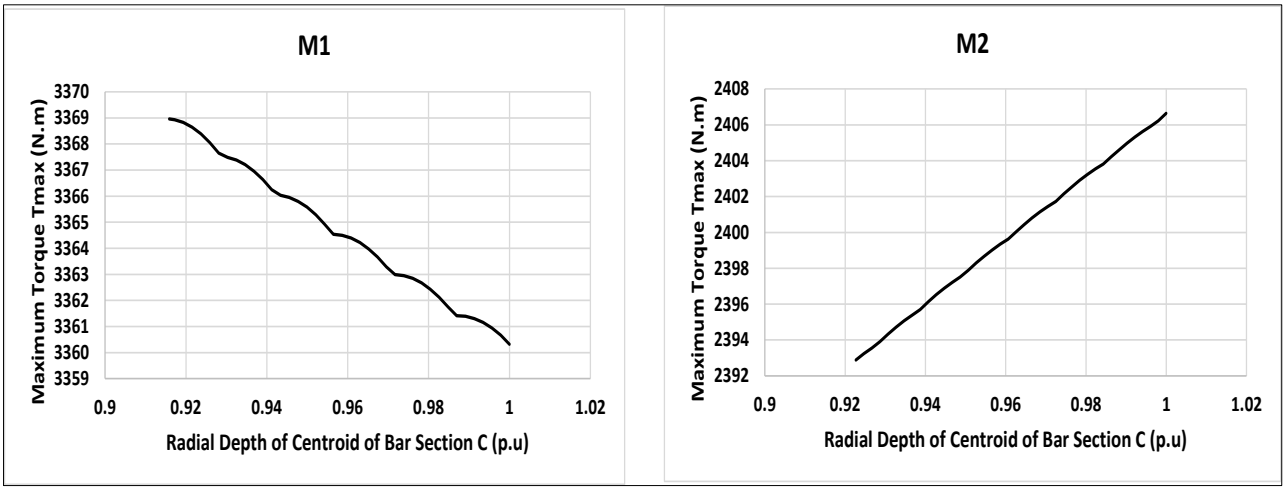

Figure 7 Influence of the radial depth of centroid on Maximum torque (Rotor bar of M1 & M2)

From the foregoing, it may be observed that the exerted influence of C on X_2 and consequently on T_{max} seem not to exist in the M2 machine; and if at all it exists, it does to a level of significance that is inferior to those of the other relevant bar parameters. While in the M1 machine, the exerted influence of C on X_2 and consequently on T_{max}, appears quite significant. It may therefore be deduced that the influence of parameter C (radial depth of bar centroid) on T_{max} is to the extent of its influence on X_2, and this influence tends to be more significant for rotor bar cross sections that have their centroid closer to the airgap as in machine M1.

4 Test and Validation

It is to be tested that the cumulative influence of all investigated variables of the rotor bar on the production of moderate slip torques in particular, could also have been largely achieved with the identified variable – C only.

To carry out this test, the experimental machine M1 was used and a reference case for two other variants of the same machine was chosen. The first variant – the base case was the case in which the dimensions of all the investigated parameters of the rotor bar were reduced together from the reference case, so as to influence torque. The second variant was the control case, in which only the radial depth of the rotor bar centroid was deliberately allowed to vary from the reference case as well – of course, this implies a corresponding change in bar cross sectional area (CSA) which by itself has no substantiated influence on T_{max}. All cases were simulated and the results are given in table 3.

Table 3 Test results

	Maximum torque Tmax (N.m)	Rotor bar top Width W (mm)	Rotor bar radial depth D (mm)	Angle of bar taper T (Degrees)	Radial depth of the centroid of bar section C (mm)	Rotor bar cross-sectional area A (sq.mm)	X2 for Moderate slip (ohms)
Reference case	3360.3235	11.60119	27.84286	9.869465	12.15599	222.594	0.0206948
Base case (W, D, T & C are varied)	3368.9628	10.48168	25.15602	9.266795	11.13309	185.6698	0.0205021
Control case (only C is varied)	3364.5341	11.60119	27.84286	9.869465	11.14533	185.8555	0.020557

On comparing the base and control cases as in fig 8 and table 3, shows that in the base case, the slot leakage flux level (typified by the X2 value) which usually governs the maximum torque level, was reduced relative to the reference case by the resultant effect of the dimensions of the geometric variables of W, D, T and C (neglecting the stator variables). The magnitude of this influence was almost equaled by the variation of only the variable C, but for the overshadowing effect of the relatively higher dimensions of the parameters D and T (supporting a high X2); which were the same for both the reference and control cases. Table 3 shows thar the difference between their respective deviations from the reference case is just about 0.13% (4.4 Nm.). Also, the control case seems to switch alignment from the base to the reference case as we move towards low speed; suggestive of the fact that the influence of C (and CSA) is getting weaker at high slip.

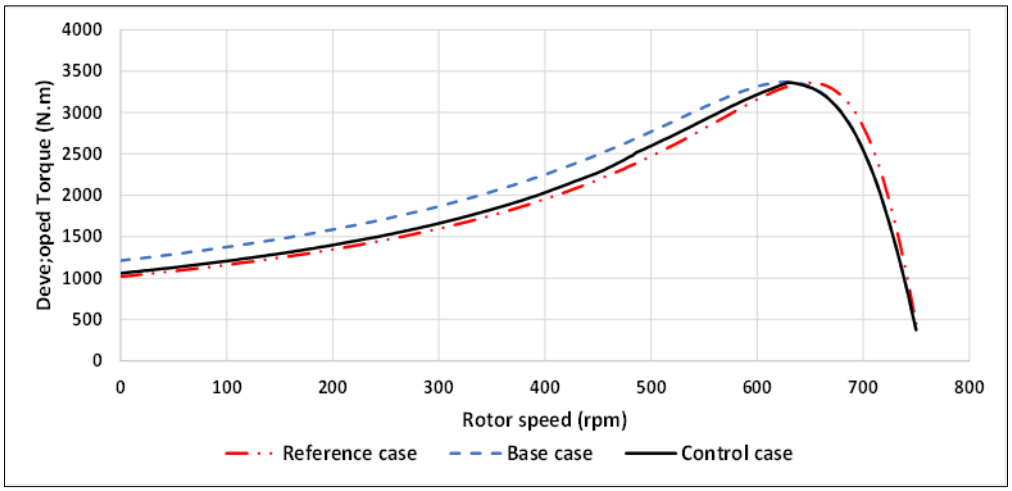

Figure 8 Test result

5 Conclusion

From the foregoing, it may be concluded that the design changes made to the radial depth of the centroid of the rotor bar cross section show significant influence on the level of the slot leakage flux and consequently on the level of maximum torque. However, this finding was observed not to be universal within the family of the three phase SCIMs; as the observed significance appears to be specific to machines that house rotor bars with cross section shaped so as to position the centroid as close to the airgap as possible. Therefore, within the accuracy bounds of the experimental methods and materials employed in this study, the designers, researchers and students working on the 3ph squirrel cage induction motor are herein presented with the centroid of the rotor bar section, as a novel influential geometric variable with potentials that could arguably prove requisite for the infeed of torque optimization algorithms/programs. Especially in cases in which it is required to make marginal modifications to theT_{max}, it would become unnecessary to introduce avoidable complexity to the engineer's design algorithms/programs and eventually, a more error prone final

solution; by inputting and adjusting all available T_{max} -influencing geometric parameters of the rotor, in the design and optimization routines, when just the centroid of the rotor bar as observed, could do the job considerably well**.**

Compliance with ethical standards

Acknowledgments

Due appreciation also goes to the following impactful personalities who in the following ways and more, have been of immense assistance: Professors O. A Ezechukwu and E. A. Anazia of the Electrical Engineering department of the Nnamdi Azikiwe University, as well as the entire staff of the department for their unassuming support. MathWorks and Microsoft conglomerates for putting together very effective virtual laboratory environments. Mr. Festus Odijie, Dr. Courage Omogbai, Dr. Femi Asekhame.

Disclosure of conflict of interest

There exists no conflict of interest whatsoever.

References

[1] Turcanu, OA., Tudorache, T. and Fireteanu, T. Influence of squirrel-cage bar cross-section geometry on induction motor performances. A paper presented at the International Symposium on Power Electronics, Electrical Drives, Automation and Motion.in Sicily, Italy. held at Taormina on the 23 – 26 May, 2006.

[2] Di Nardo, M., Marfoli, A., Degano, M., Gerada, C. and Chen, W. Rotor design optimization of squirrel cage induction motor - part II: results discussion. IEEE. 1 – 9. Doi: 10.1109/TEC.2020.3020263. 30 July, 2021.

[3] Maloma, E., Muteba, M. and Nicolae, D., Effect of Rotor bar Shape on the Performance of Three Phase Induction Motors with Broken Rotor Bars. 2017 international conference on optimization of electrical an electronic equipment (OPTIM). 364 – 369. Doi:10.1109/OPTIM.2017.7974997. 17 September, 2021.

[4] Vukosavic NS. Electrical Machines. Springer New York Heidelberg Dordrecht London. ISBN: 978-1-4614-0400-2 (www.springer.com) 2013. DOI: 10.1007/978-1-4614-0400-2. Pp. 365 – 472.

[5] Boldea, I. and Nasar, S. A. (2010). The Induction Machine Handbook. Washington, D.C: CRC Press, Taylor & Francis Group. PP. 447 – 473.

[6] Fireteanu, V. Squirrel-Cage Induction Motor with Intercalated Rotor Slots of Different Geometries. XIII International Symposium on Electromagnetic Fields in Mechatronics, Electrical and Electronic Engineering, September, 2007. DOI: 10.3233/978-1-58603-895-3-284.

[7] Purwanto, W., Sugiarto, T., Maksum, H., Martias, M., Nasir, M. and Baharudin, A. (2019). Optimal design of rotor slot geometry to reduce rotor leakage reactance and increase starting performance for high-speed spindle motors. Advances in Electrical and Electronic Engineering. 17 (2) 2019. 96 – 105, Doi: 10.15598/aeee.v17i2.3170.

[8] Cochran, PL. Polyphase Induction Motors. Analysis Design and Application. Marcel and Dekker. NY. USA 1989. ISBN 0-8247-8043-4. Pp. 427 – 585.

[9] Akhtar, MJ., Behera, RK. and Parida, SK. Optimized Rotor Slot Shape for Squirrel Cage Induction Motor in Electric Propulsion Application. IEEE 6th india international conference on power electronics (IICPE) 2014. 1 – 5. Dol: 0.1109/IICPE.2014.7115846.

[10] Yetgin, AG. and Turan, M. Effects of rotor slot area on squirrel cage induction motor performance. International Journal of Innovative Science, Engineering & Technology 2016. 3 (11),105 – 109. Retrieved from www.ijiset.com.

[11] Ho, S. (1996) Analysis and Design of AC Induction Motors With Squirrel Cage Rotors. Doctoral Dissertations. University of New Hampshire, Durham 1996. Retrieved from: https://scholars.unh.edu/dissertation/1909.

[12] Theraja, BL., Theraja, AK., A Textbook of Electrical Technology. S. Chand Publishing 2008.

[13] Gupta, JB. Theory and Performance of Electrical Machines. S. K. Kataria and Sons 2013. New Delhi, India. Www.skkatariaandsons.com. Part III, Pp. 359 – 439.

[14] De Brabanter, K., Karsmakers, P., Ojeda, F., Alzate, C., De Brabanter, J., Pelckmans, K., De Moor, B., Vandewalle, J., and Suykens, JAK. LS-SVMlab Toolbox User's Guide version 1.8. ESAT-SISTA Technical Report 10-146. http://www.esat.kuleuven.be/sista/lssvmlab/.

[15] Omogbai, ON., Anazia, AE., Anionovo, UE. Exploring the Influence of Rotor Bar Taper Angle on Breakdown Torque using Machine Learning. International Journal of Advances in Engineering and Management 2023. Volume 5, Issue 1, pp: 249-255 www.ijaem.net.

[16] Chapman, S. J. (2005). Electric Machinery Fundamentals. Fourth Edition. The McGraw-Hill Companies. Inc. ISBN 0-07- 246523—9, www.mhhe.oom. Pp. 380 =472.

[17] Ibrahim, S. Centroid and Center of Mass of The Composite Bodies. 2014. https://www.researchgate.net/publication/307605237. DOI: 10.13140/RG.2.2.24991.36002